GEOPHYSICAL RESEARCH LETTERS, VOL. 19, NO. 14, PAGES 1455-1458, July 24, 1992

REMOTE-SENSING OBSERVATIONS OF F-REGION ION DRIFT VELOCITIES USING DYNAMICS EXPLORER-2 DOPPLER MEASUREMENTS OF THE $O^+(^2P)$ λ732.0 nm EMISSION

S.S. Carr and T.L. Killeen

Space Physics Research Laboratory
Department of Atmospheric, Oceanic, and Space Sciences, The University of Michigan

W. Robin Coley

Center for Space Sciences
University of Texas at Dallas, Richardson, TX 75083-0688

Abstract. Limb-scan observations of Doppler line profiles from the $O^+(^2P)$ λ732.0 nm emission at F-region altitudes, made with the Fabry-Perot interferometer (FPI) on the Dynamics Explorer-2 (DE-2) spacecraft, have been analyzed to provide measurements of the meridional component of the ion convection velocity along the instrument line-of-sight. The initial DE-2 results presented here demonstrate the first spaceborne use of the remote-sensing Doppler technique for measurements of ionospheric convection. The FPI meridional ion drift measurements have been compared with nearly simultaneous in-situ ion drift measurements from the Retarding Potential Analyzer (RPA) on DE 2. Once allowance is made for the temporal lag between the in-situ and remote measurements, the results from the two techniques are in good agreement. The results of a simulation study demonstrate that the spaceborne interferometric technique has future utility for 2-D imaging of the quasi-instantaneous ion convection pattern.

Introduction

Ground-based Doppler measurements of F-region ion drift velocities, using the $O^+(^2P)$ λ732.0 nm multiplet emission, have been shown to be possible when the emission is sufficiently intense during nighttime hours [Smith et al., 1982; McCormac, 1984]. This condition is satisfied at times in the polar cusp, polar cap, and other high-latitude auroral regions. Up to the present time, however, no spaceborne Doppler measurements of ion drift have been reported. The potential advantage of spaceborne optical measurements is twofold. First, the large geometric limb-intensity enhancement leads to improved sensitivity and/or smaller instruments for the same accuracy of measurement. Second, the ability of a baffled spaceborne limb scanner to discriminate against Rayleigh-scattered sunlight enables a daytime capability that takes advantage of the much brighter daytime O^+ emission.

The Dynamics Explorer-2 (DE-2) Fabry-Perot interferometer (FPI) [Hays et al., 1981; Killeen et al., 1982] was the first space-borne instrument with adequate spectral resolution to measure remotely thermospheric winds from the Doppler shifts of atmospheric emissions. The FPI Doppler-line-profile analysis technique has been discussed by Killeen and Hays [1984] and a summary of many of the geophysical results can be found in the review by Killeen and Roble [1988] and references therein.

One of the optical filters used in the DE-2 FPI instrument was chosen to enable Doppler measurements of the ionospheric O^+ λ732.0 nm emission. While the primary objective of the FPI was the measurement of neutral winds and temperatures, the 732.0 nm filter was used routinely in a background, time-shared mode and a large data base of over 1000 orbits exists. These data have now been reduced to provide ion drifts and ion temperatures along the instrumental line-of-sight. We present initial results of the DE-2 FPI O^+ Doppler-line profile measurements and evaluate the technique in terms of its capability as a remote sensor of ionospheric convection. The results of a validation study, using simultaneous ion drift measurements from the DE-2 Retarding Potential Analyzer, RPA [Hanson et al., 1981; Heelis et al., 1986], demonstrate that reliable remotely-sensed ion drift velocities are recoverable.

The O^+ λ732.0-733.0 nm multiplet atmospheric emission is produced in daytime, twilight, and aurora and is the result of the metastable transition between excited ^2P and ^2D states of O^+ ions. Metastable $O^+(^2P)$ ions have a lifetime of 4.57 seconds and a branching ratio of 0.781 for the ^2P-^2D transition [Yee, 1980]. Since the time taken for a newly-created ion to drift with the bulk ion population in the ExB direction is very short (essentially given by the gyroperiod), it may be assumed that the Doppler shift of the emitted light is representative of the convection velocity. $O^+(^2P)$ ions are primarily produced in the atmosphere by photoionization of neutral atomic oxygen by solar EUV radiation at wavelengths less than 66.6 nm. A secondary source of $O^+(^2P)$ ions is electron impact ionization, with an ionization threshold energy of 18.61eV. $O^+(^2P)$ ions are lost by quenching or spontaneous emission. Spontaneous emission of the ions to lower states is given by:

$$O^+(^2P) \xrightarrow{A_\lambda} O^+(^2D,^2S) + h\nu; \qquad A_\lambda = 0.219\ s^{-1}$$

The DE-2 O^+ λ732.0 nm filter was designed to measure the $O^+(^2P$-$^2D_{5/2})$ doublet emission at 732.0 nm. We first review the nature of the remote-sensing experimental technique. Measured Doppler line profiles and a typical measured volume emission rate profile are shown. We then present examples of the remote ion drift measurements and describe the results of the validation comparison between the FPI and RPA. Finally,

Paper number 92GL00627
0094-8534/92/92GL-00627$03.00

we present the results of a simulation study to demonstrate the capability of the remote-sensing technique for 2-D imaging of the polar ion convection pattern.

DE-2 FPI (O^+) λ732.0 nm Emission Observations

The DE-2 FPI observations were all carried out in the meridional (north-south) direction. The instrument incorporated a twelve channel image-plane detector (IPD) that had a quantum efficiency of 2.8% at 732.0 nm. At 732.0 nm and 283K (the instrumental operating temperature), the O^+ filter had a peak transmission of 47% and a 1.0 nm FWHM bandpass. The FPI viewed the atmospheric limb cyclically at various tangent heights, using an on-board scanning mirror. The instrument performed a high-resolution spectral analysis of the 732.0 nm emission by measuring the geometry of the interference fringe patterns imaged onto the IPD. This analysis allowed the Doppler line profile of the $O^+(^2P)$ emitting species to be characterized. The individual Doppler spectrograms, in turn, enabled meridional ion drifts, ion temperatures, emission surface brightnesses, and continuum (background) brightnesses to be determined using the method of Killeen and Hays [1984]. The FPI was capable of measurement accuracies of ~5 m/s and ~10K for meridional ion drift and ion temperature, respectively. Accuracies for individual measurements were dependent on the respective surface brightness and the chosen integration time.

Figure 1 depicts individual, bin-averaged 732.0 nm spectrograms obtained on orbit 8227. The modulation seen in each spectrogram represents the discretely-sampled Doppler line profile of the emission. The etalon gap was chosen such that the individual lines of the 732.0 nm doublet almost exactly overlap on the image plane. The free spectral range (FSR) at 732.0 nm was 0.021 nm and there were 11.59 channels per FSR. The Doppler shift corresponding to the width of one channel is therefore equivalent to a wavelength interval of 0.0018 nm, which corresponds to an ion drift of ~750 m/s. The spectrograms shown represent convolutions of the Doppler source function, characterized by the ambient ion drift and temperature, and the instrument function. These two functions were deconvolved during the analysis procedure and the resulting line-of-sight drift and brightness results inverted using the technique of Nardi [1991] to derive true altitude profiles. In practice, the "inverted" ion drifts were found to be almost indistinguishable from the line-of-sight drifts in the tangent-point altitude range 200 - 400 km due to the sharply peaked nature of the contribution functions [c.f., Killeen et al., 1982; Nardi, 1991].

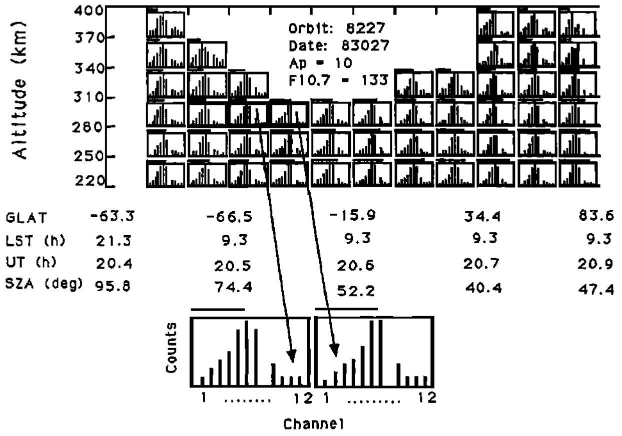

Fig. 1. Examples of FPI-measured O^+ λ732.0 nm Doppler spectrograms from DE-2 orbit number 8227. The individual spectrograms depict the count rate (counts per second) measured at each channel of the instrument, with the exception of channel 8. The horizontal bar above each spectrogram denotes relative intensity.

Each spectrogram in Figure 1 is plotted with respect to the altitude and latitude of the tangent point to the Earth's surface along the instrumental line-of-sight. Relative ion drifts can be discerned in Figure 1 by the evident sideways motion of the peak centroid from spectrogram to spectrogram; the enlargement of the two spectrograms from ~280 km illustrates this point. The ion drift measurement is obtained by determination of the Doppler line centroid using the non-linear least squares fitting technique of Killeen and Hays [1984]. The length of the horizontal bar given at the top of each spectrogram provides a relative (linear) intensity scale for the O^+ emission. Channel 8 has been removed from the DE-2 spectrograms and the analysis procedures, since that channel had a non-stochastic noise component. Above ~200 km, the relative intensity of the λ732.0 nm emission increases to peak at ~300 km. We have developed a detailed aeronomical model for the 732.0 nm emission as an aid in the analysis of the FPI data. This model includes consideration of all the chemical sources and sinks discussed above and will be described in a forthcoming paper.

An example of a λ732.0 nm volume emission rate (VER) profile, as determined from the inversion of the measured line-of-sight brightnesses, is shown in Figure 2. The VER data are compared with the calculations from our aeronomical model for equivalent geophysical conditions, with good evident agreement. The VER reduction below the peak (at ~ 300 km) is due to an increase in quenching. The VER decrease above

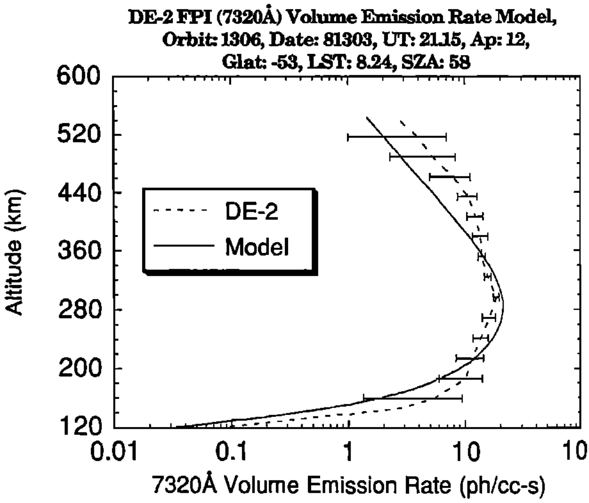

Fig 2. Inverted O^+ λ732.0 nm volume emission rate profile for orbit 1306 of DE 2. The measured profile is compared with a theoretical model, based on evaluation of $O^+(^2P)$ sources and sinks for equivalent geophysical conditions.

the peak is due the combination of decreasing electron and atomic oxygen number densities.

For the purposes of absolute ion drift measurements, a zero-velocity calibration is necessary. This calibration was obtained in flight by averaging daytime observations at equatorial latitudes from a total of 59 orbital passes and assuming zero low-latitude meridional ion drift on the average. In addition, calibrations to correct for FPI instrumental drift were carried out twice per orbital pass, using the on-board calibration lamp source. The offset error associated with these calibrations is estimated to be < 15 m/s. The quoted statistical errors in the measured ion drifts are determined from the diagonal elements of the matrix used in the non-linear least squares fit. Overall systematic errors, including spacecraft pointing errors, instrumental drift and offset errors are estimated to be <25 m/s.

Comparisons Between FPI and RPA Meridional Ion Drift Measurements

The FPI ion drift measurements were compared with simultaneous measurements of the RPA to validate the remote-sensing technique. The RPA provided measurements of meridional ion drift velocity using a well-proven and more conventional in-situ technique. The accuracy for RPA ion drift measurements was ~10%. In order to make a comparison between the observed ion drifts, an adjustment was made to allow for the spatial difference between the physical volumes of space sampled by the remote and in-situ techniques. The field of view of the FPI varied from 5°-15° below the local horizontal. Hence, the distance from the spacecraft to the tangent point to the Earth's surface along the line-of-sight varied between ~500 and 1700 km. For each measurement, therefore, a separate temporal lag (~1-3 minutes) was applied to the RPA measurements such that the comparison was always between RPA measurements made directly above the sampled volume of the (prior) FPI measurement. Inherent in this data handling approach is the assumption that no significant changes in ion drift occur during the time delay for DE 2 to reach the locality of the tangent point of any given FPI measurement. While this assumption is questionable at high latitudes and during disturbed conditions, the level of agreement seen between the two techniques justifies its use.

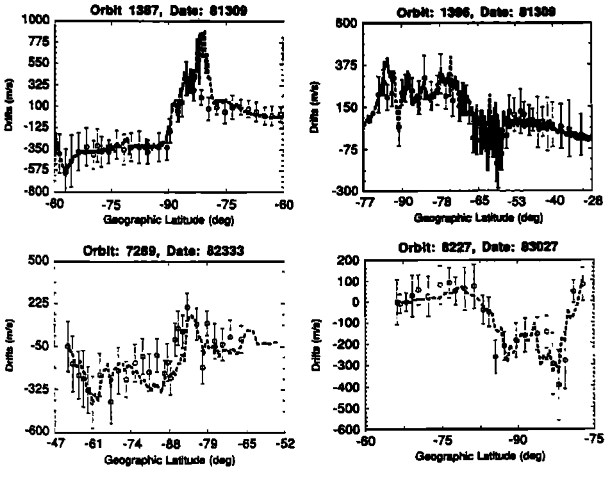

Fig. 3. Meridional ion drifts measured by the FPI (circles) and the RPA (dashed lines) on DE 2 for four specified orbital passes. FPI errors are standard deviations from the mean.

A further assumption was necessary concerning the altitude invariance of the meridional ion drift. The FPI measurements were bin averaged using data obtained within the range of 200-400 km tangent point altitudes. The RPA measurements were made at satellite altitude. The assumption was made that the convection electric field remains constant with decreasing altitude down to ~150 km where collisional effects first become important. With this assumption, the remote FPI drift measurements may be directly compared with the in-situ observations at satellite altitude.

Figure 3 shows four examples of "simultaneous" FPI and RPA ion drift measurements for selected polar passes of DE 2. The FPI integration time period was ~30 seconds. As can be seen, the independent measurements are in good agreement, for the most part within specified errors. Significant discrepancies are ascribed to the tendency of the remote FPI measurement to smear out large shears due to the relatively long spatial integration path length of the measurement (~300-500 km at the limb) and to possible temporal changes occurring on shorter time scales than the temporal lag discussed above.

Simulated Convection Pattern Imaging

The validated performance of the DE-2 FPI as a remote spaceborne monitor of ionospheric convection opens the possibility that remote sensing methods can be used to image the quasi-instantaneous, high-latitude convection pattern, as discussed recently by Minow and Smith [1990]. In order to demonstrate the potential of this 2-D imaging technique based on the results of the present paper, we have conducted a quantitative simulation study using a combination of our aeronomical model of the O^+ $\lambda 732.0$ nm emission, a model of polar ionospheric convection, and an instrument function similar to that of the DE-2 FPI.

In the simulation study, we assumed a polar-orbiting satellite at an altitude of 600 km equipped with an FPI with similar characteristics to the DE-2 FPI, but viewing the O^+ $\lambda 732.0$ nm emission at various tangent point altitudes in four azimuthal directions at ±45° and ±135° to the satellite velocity vector. In this mode, the vector ion drift can be derived by combining the various observations and assuming temporal invariance of the pattern over periods of ~5 minutes. By adjusting the horizon scan angle, it is possible to obtain several sets of vector measurements at different horizontal spacings from the satellite. The simulated spectrograms were calculated by integrating all emission contributions along each field of view and assigning an ion drift to each contribution. Poisson noise was added to increase the realism of the simulation. The simulated instrument was assumed to be 12 times more sensitive than the DE-2 FPI (consistent with modern CCD detection capabilities). The horizontal ionospheric convection pattern (zero vertical drift) was based on output from the model of Heelis et al. [1982] and was assumed to be invariant in magnetic coordinates.

Figure 4 shows the results of the simulation. Figure 4a represents the convection pattern used as input to the calculation. Figure 4b depicts the recovered ion drifts after the

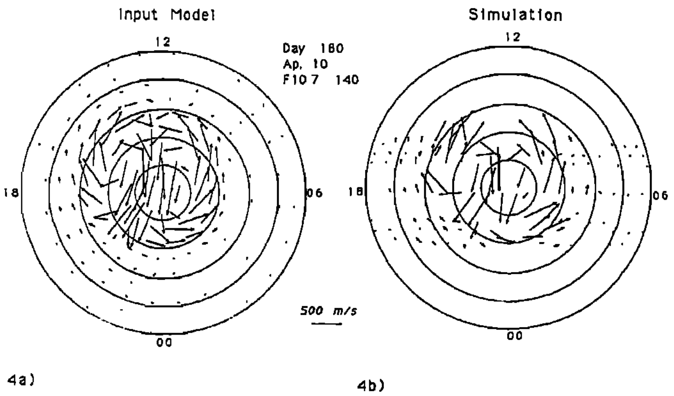

Fig. 4. a) Ion drift pattern used as input to the convection-imaging simulation. The pattern is in geographic polar coordinates, with the outer circle at 40° N latitude. b) Recovered ion drift vectors from the simulated FPI measurements.

complete forward and reverse calculation, including effects of spatial smearing, noise, velocity inversion, instrument sensitivity, viewing geometry, and emission morphology. It was assumed that an in-situ sensor provided drift measurements along the satellite track. The integration time period was assumed to be 30 seconds for each observation and the calculated statistical error on a single dayside measurement was ≤5 m/s. Remote measurements of the ion drift using the interferometric technique were calculated at several off-track tangent-point altitudes corresponding to different zenith angles for the fields of view. For the purposes of the plot, three such sideways views to each side of the spacecraft were assumed, yielding a swath of information containing 6 independent vector measurement sets at different lateral distances from the spacecraft orbital track. The angular extent of the overall swath is therefore ~40°, enabling both cells of the convection pattern to be clearly imaged.

As can be seen, the recovered pattern agrees well with the input pattern, demonstrating that quasi-instantaneous ionospheric convection patterns can be imaged over periods of ~15 minutes, the time taken for a polar-orbiting spacecraft to traverse the convection region. Such images could be collected twice per orbit, once in each hemisphere, with greater coverage of the summer polar region where emission rate intensities are greater. The evident good agreement between input and simulation makes this technique very attractive for the routine monitoring of high-latitude convection. It is suggested that temporal sequences of such images could provide definitive information concerning convection cell numbers and geometries for differing geophysical situations, with a spatial resolution of ~1-3° latitude, depending on satellite altitude and viewing conditions.

Conclusions

First results of remotely-sensed ion drifts from DE 2 have been presented. The remote ion drift measurements have been validated using independent in-situ RPA observations. Simulations have demonstrated the use of the technique for the routine monitoring of 2-D ionospheric convection. While the statistical errors associated with the remote measurements are larger than those typically associated with conventional in-situ techniques, the technique is powerful in terms of its potential for remote imaging of the quasi-instantaneous polar ionospheric convection pattern.

Acknowledgements. This work was supported by NASA grants NAG5-465 and NAGW-1535. S. S. Carr is funded by the US Air Force. The authors are grateful to Drs. W.B. Hanson and R.A. Heelis for providing the RPA data.

References

Hanson, W. B., R. A. Heelis, R. A. Power, C. R. Lippincott, D. R. Zuccaro, B. J. Holt, L. H. Harmon, and S. Sanatani, The retarding potential analyzer for Dynamics Explorer-B, Space Sci. Instrum., 5, 503, 1981.

Hays, P.B., T.L. Killeen and B.C. Kennedy, The Fabry Perot Interferometer on Dynamics Explorer, Space Sci. Instr., 5, 395, 1981.

Heelis, R. A., J. K. Lowell, and R. W. Spiro, A model of the high-latitude ionospheric convection pattern, J. Geophys. Res., 87, 6339, 1982.

Heelis, R. A., P. H. Reiff, J. D. Winningham, and W. B. Hanson, Ionospheric convection signatures observed by DE 2 during northward interplanetary magnetic field, J. Geophys. Res., 91, 5817, 1986.

Killeen, T. L. and R. G. Roble, Thermosphere Dynamics driven by magnetospheric sources: contributions from the first five years of the Dynamics Explorer program, Rev. Geophys. Space Phys., 26, 329-367, 1988.

Killeen, T.L. and P.B. Hays, Doppler Line Profile Analysis for a Multichannel Fabry-Perot Interferometer, Applied Optics, 23, 612, 1984.

Killeen, T. L., P. B. Hays, N. W. Spencer, and L. E., Wharton, Neutral winds in the polar thermosphere as measured from Dynamics Explorer, Geophys. Res. Lett., 9, 957, 1982.

McCormac, F. G., An optical investigation of ion and neutral motions in the polar thermosphere, PhD Thesis, Ulster Polytechnic, April, 1984.

Minow, J. I., R. W. Smith, Optical Remote Sensing of the Ion Convection Pattern in the High-Latitude Ionosphere From a Polar Orbiting Satellite, EOS abstract, Trans. of the AGU, 71, 1486, 1990.

Nardi, B., An Inversion Technique to Recover Lower Thermospheric Winds from Space-Borne Remote Measurements of (OI) 5577Å, PhD Thesis, The University of Michigan, 1991.

Smith, R. W, G. G. Sivjee, R. D. Stewart, F. G. McCormac, and C. S. Deehr, Polar Cusp ion drift studies through high-resolution interferometry of O^+ 732.0 nm emission, J. Geophys. Res., 87, 4455, 1982.

Yee, J.H., A Theoretical and Experimental Study on the Atomic Oxygen Corona in the Earth's Atmosphere, PhD Thesis, The University of Michigan, 1980.

S. S. Carr, T. L. Killeen, Space Physics Research Laboratory, Department of Atmospheric, Oceanic and Space Sciences, The University of Michigan, 2455 Hayward, Ann Arbor, MI 48109.

(Received: February 17, 1992;
accepted: March 9, 1992)